

## Determination of Maximum Wind Power Penetration Considering Wind Turbine Fast Frequency Response

Rakhshani, Elyas; Rueda Torres, Jose Luis; Palensky, Peter; van der Meijden, Mart

**DOI**

[10.1109/PTC.2019.8810492](https://doi.org/10.1109/PTC.2019.8810492)

**Publication date**

2019

**Document Version**

Final published version

**Published in**

2019 IEEE Milan PowerTech

**Citation (APA)**

Rakhshani, E., Rueda Torres, J. L., Palensky, P., & van der Meijden, M. (2019). Determination of Maximum Wind Power Penetration Considering Wind Turbine Fast Frequency Response. In *2019 IEEE Milan PowerTech* (pp. 1-6). Article 8810492 IEEE. <https://doi.org/10.1109/PTC.2019.8810492>

**Important note**

To cite this publication, please use the final published version (if applicable). Please check the document version above.

**Copyright**

Other than for strictly personal use, it is not permitted to download, forward or distribute the text or part of it, without the consent of the author(s) and/or copyright holder(s), unless the work is under an open content license such as Creative Commons.

**Takedown policy**

Please contact us and provide details if you believe this document breaches copyrights. We will remove access to the work immediately and investigate your claim.

***Green Open Access added to TU Delft Institutional Repository***

***'You share, we take care!' - Taverne project***

**<https://www.openaccess.nl/en/you-share-we-take-care>**

Otherwise as indicated in the copyright section: the publisher is the copyright holder of this work and the author uses the Dutch legislation to make this work public.

# Determination of Maximum Wind Power Penetration Considering Wind Turbine Fast Frequency Response

Elyas Rakhshani,

Jose Luis Rueda Torres, and Peter Palensky

Department of Electrical Sustainable Energy  
Delft University of Technology (TUD), Netherlands

Mart van der Meijden

TenneT TSO B.V,  
Arnhem, Netherlands

**Abstract**—This paper presents a study based on sensitivity analysis to investigate the impact of fast frequency response (FFR) capability of type 4 wind turbine units on the overall frequency performance of interconnected power systems with low inertia. FFR capability is implemented by means of a control loop for inertia emulation (IE), which is superimposed on the active power control channel of the machine side converter of the wind turbine. All parameters of IE are assessed via sensitivity analysis to ascertain their influence on the system frequency performance within the time window of the frequency containment period. Both individual and collective response of the wind turbines are assessed to determine if the penetration level of wind power can be increased by customizing IE with the best parameter values found via sensitivity analysis. Numerical results, obtained by using a 3-area benchmark power system, illustrate the degree of increase in wind penetration level that can be achieved when choosing a suitable combination of wind turbine locations and considering suggested settings for IE.

**Index Terms**—Primary frequency control, fast frequency response, inertia emulation, MIGRATE, wind turbine, wind power plant integration.

## I. INTRODUCTION

From recent studies, it can be concluded that the influence of reduced inertia on frequency stability is generally considered as the main challenge for system operators [1].

Systems with low inertia are the consequence of phase out of conventional power plants with synchronous generators due to increasing penetration of renewable energy-based generation such as solar photovoltaic systems and wind power plants. Considering the variable nature of this kind of power electronic interfaced power plants, additional measures like addition of energy storage devices, and supplementary control loops to facilitate fast frequency response – FFR (i.e. fast active power injection), are important to avoid unacceptable frequency deviation in the frequency containment period (time window of 10 s from the occurrence of an imbalance) [1].

FFR is essentially a mechanism to quickly regulate the active power injection to mitigate frequency variations in low inertia systems. Since it overlaps with the time window of the

inertial response of conventional synchronous generators (0.5s from the occurrence of active power imbalance), some authors use the alternative term ‘inertia emulation’ (IE). In other words, the inertia emulation can be considered as a subset of FFR, which contains different responses based on the frequency evolution over time and the so-called rate of change of frequency (RoCoF) [2].

The actual source of energy for emulating inertia is stored in systems behind power electronic interfaces, such as batteries, and rotating masses in wind turbines. A supplementary control loop for IE enables the wind turbine to release the stored kinetic energy within 10 s to arrest the frequency deviation [3]-[4]. Existing literature shows that IE control can be implemented in different ways, ranging from de-loading technique [3], inertial based control [5]-[7], to proportional (droop) based controls [8]-[11].

The de-loading strategy aims at ensuring a reserve margin by shifting the wind turbine's operating point from its optimal power. This strategy can be superimposed in either the speed control or the pitch angle control of a wind turbine [3].

The inertial based control uses a derivative term of frequency to emulate inertia like in conventional power plants. Whereas the droop based control regulates the active power output from a wind turbine in a proportional manner w.r.t. the measured frequency change. Several studies have shown that this type of control greatly improves the frequency nadir as well as the frequency recovery process following imbalances [8]-[10].

It is worth mentioning that, in the inertial based control, if the derivative based controller reverses the direction of the power, modification of power reference due to control action, signal after the frequency reaches its limit value, the wind turbine will require additional control actions to recover to its optimum operating condition. In this case, additional droop based control is used as a complementary control action to produce a change in the power reference, extracted wind power, in proportion to the system frequency deviation. Therefore, a combination of different methods like proportional (droop) and derivative controls seems to be effective as reported in [12]-[14].

---

This research was carried out as part of the MIGRATE project. This project has received funding from the European Union's Horizon 2020 research and innovation program under grant agreement No 691800.

According to the current state of the art, droop control is easy to implement and may allow to achieve good damping and improved frequency recovery time [8]-[10], whereas de-loading strategies are not economic, entail less optimal performance, and they can introduce abrupt variations of torque [3]. Furthermore, the application of derivative control alone is not recommendable, due to its limitation in terms of practices and its noise amplification [3].

Existing works on IE are devoted to controller design considering a single wind turbine or a small set of wind turbines, which is usually connected to a small-size system. Nevertheless, detailed analysis on the impacts of IE parameters and the location of wind turbines equipped with IE is needed to determine the maximum penetration level of wind turbines that does not entail risk of frequency instability. This paper addresses this gap by performing sensitivity analysis, based on time-domain simulations, to assess the influence of IE control parameters on the system frequency performance in the frequency containment period. By evaluating individual and collective behavior of wind turbines, the goal is to identify an optimal combination of wind turbine locations with suitable settings for IE controller.

The time-domain simulations consider type 4 wind turbines, equipped with droop based IE. Important aspects of inertia emulation limits, the importance of activation time (triggering of IE controller), wind power plant combinations (each one equipped with IE controller), recommendable ranges for each control parameter, and the maximum level of penetration for the studied 3-area benchmark power system are presented and discussed.

## II. FAST FREQUENCY RESPONSE OF WIND POWER

The implementation of the wind turbine model and the benchmark system, and the time domain simulations are done by using DIgSILENT PowerFactory 2016 SP3. Several scripts were developed in Python 3.4™ and Matlab R2016b® to automate the IE parameter variations and the simulation of different operational scenarios and network topologies

### A. Wind Turbine Overall Control

A generic model of type 4 wind turbine is used in this research work. The static generator element of PowerFactory is used to represent the wind turbine as a controllable voltage source. The control scheme attached to the static generator is developed based on IEC 61400-27 standard [11]. Additional controllers were added as shown in Fig. 1 to consider IE and modified P and Q control channels which illustrates the overall structure of the adopted wind turbine control.

The type 4 wind turbines are connected to the transmission network following the wind power plant layout shown in Fig. 2.

### B. Inertia Emulation Controller

The general structure of IE controller is presented in Fig. 3. The IE controller is the improved (with more details of time duration logics and IE thresholds for triggering and maximum power emulation) version of ENERCON IE [11], which reacts to a drop in system frequency by temporarily increasing the wind turbine active power output. The energy

for this increase is drawn from the rotating masses of the wind turbine.

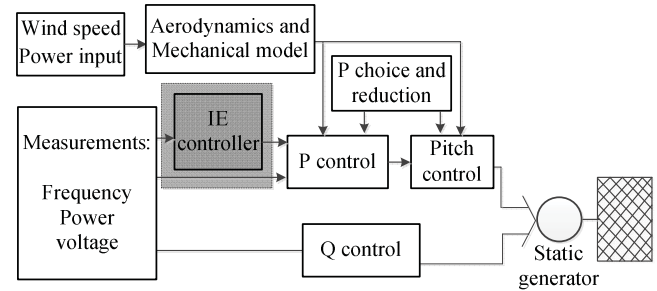


Figure 1. Controllers considered in the model of type 4 wind turbine. The blocks with white background correspond with the generic control loops defined in IEC 61400-27 standard, whereas the blocks highlighted with light grey are additions to consider inertia emulation.

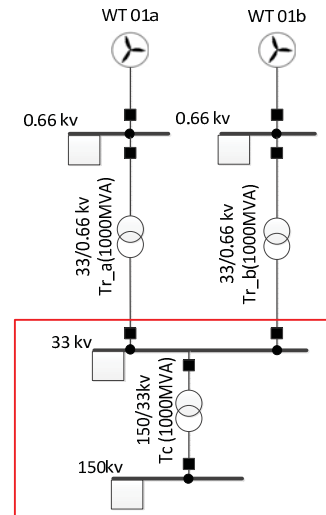


Figure 2. Network interface of a wind power plant with type 4 wind turbines.

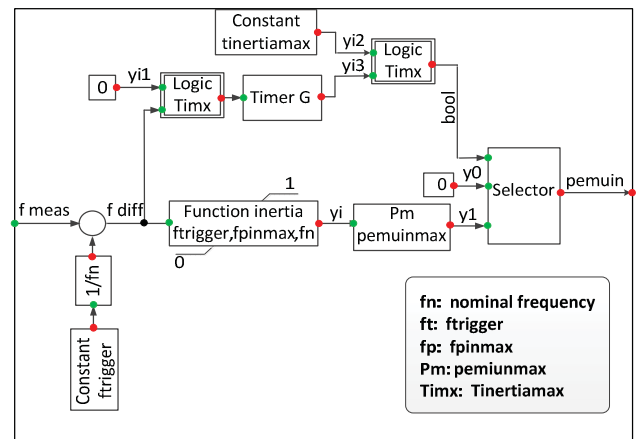


Figure 3. Implemented IE controller type 4 wind turbine.

In this control approach, when the frequency drops below a certain value  $f_{inertia,trigger}$  (named as  $f_t$ ), the inertia emulation (IE) block is activated. When the frequency

reaches an even lower value ( $f_p$ ), the maximal allowed power through emulated inertia ( $p_{inert,max}$ ) is released.

From Fig. 3 (cf. control loop in the middle of the block diagram), it can be inferred that there is a linear dependency (defined by the proportional gain  $P_m$ ) between frequency and the additional power signal ( $p_{inert}$ ), if the frequency deviation is between 1 and 0. During this interval, the following formula is used:

$$P_{inertia}(t) = \frac{f_{inertia,trigger} - f(t)}{f_{inertia,trigger} - f_{inertia,max}} P_{inertia,set} \quad (1)$$

$$= \frac{f_{diff}}{f_{inertia,trigger} - f_{pinmax}} P_m$$

where  $P_{inertia,set}$  is the maximum power increase command as a proportion of nominal power of the wind turbine, and  $f_{inertia,max}$  is the frequency threshold (named  $F_p$ ) at which the maximum emulated inertia power will be released. The value of  $P_m$  can be set between 10% to 20% of the nominal wind turbine active power [11] and [16].

### III. SENSITIVITY BASED APPROACH FOR FREQUENCY MITIGATION MEASURE

Fig. 4 shows the proposed approach for sensitivity analysis to tune and determine the maximum penetration level of wind power plants, as a function of IE parameters and selected wind power plant locations. The procedure considers a given power system model with a number of wind power plants associated to a given penetration level, an initial set of IE control parameters (cf. Table I), a selected disturbance (e.g. generator outage), and a selected operational scenario (e.g. peak load demand and corresponding generation dispatch and network topology) as inputs. Next, for each wind power plant equipped with IE, an iterative process (implemented in a Python script) is performed to sweep over each IE control parameter, while keeping the other parameters fixed. Next, time domain (RMS) simulations are executed in PowerFactory. A Matlab script is then executed to extract the time data series of relevant measurements (e.g. grid frequency) to assess the performance of the system (calculation of RoCoF and Nadir). The objective is to identify the value of each IE control parameter, which enhances the FFR of the wind power plant. The iterative process is applied to individually tune each single wind power plant. Afterwards, the penetration can be increased, and by applying the same procedure, different combinations of wind power plants (each with its own IE parameters) with IE activated are assessed to determine the best combination that entails satisfactory values of Nadir. The maximum penetration level is found when RoCoF or Nadir thresholds cannot be met.

This procedure is applied to a modified version of the PST-16 benchmark system [16] shown in Fig. 5. In order to analyze the impacts of inertia emulation controller with high level of wind power penetration, different operational scenarios are considered. In these operational scenarios, by replacing different synchronous generators with wind parks (cf. Fig. 5), different penetration levels, 35%, 41%, and 50%, has been used. While the system with 50% of penetration was chosen as the base case scenario. Further details are presented in the next section.

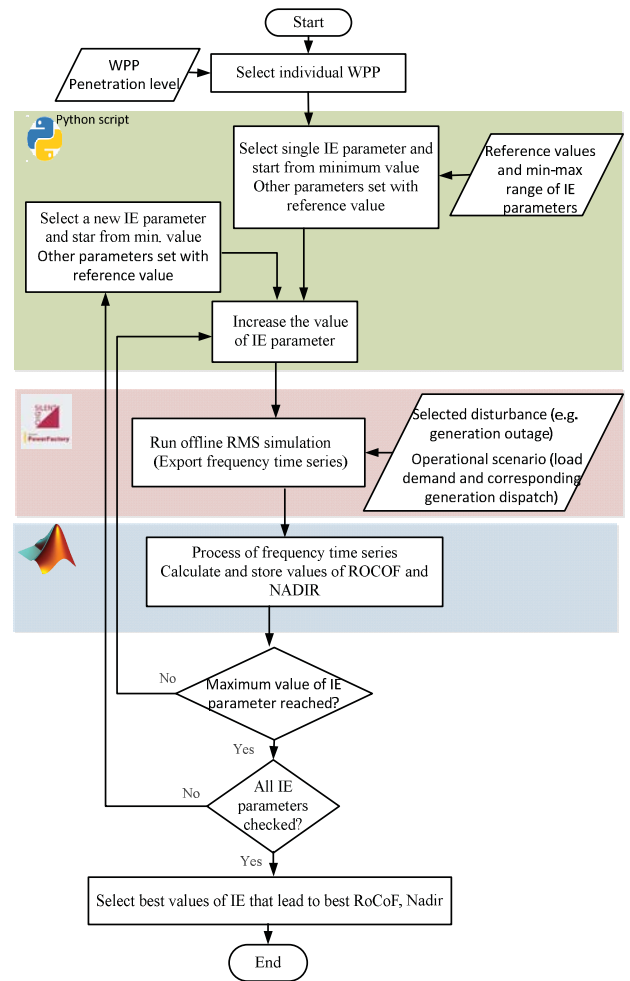


Figure 4. Procedure for tuning of IE control parameters.

### IV. RESULTS AND DISCUSSIONS

In this section, the procedure defined in Sections II and III is applied to a modified version of the PST-16 benchmark system [16]. The single line diagram of the system is shown in Fig. 5 highlighting the added wind power plants, which are used to create different penetration levels. A worst case active power imbalance is created by considering the outage of the biggest synchronous generator (A1aG, which entails the losing of 1000 MWs) at  $t = 5$  s. The total demand of the system is 15480 MW. The generation dispatch is adjusted to consider different penetration levels of wind power generation. As the base scenario, it is considered that 50% of the demand is supplied by wind power plants.

The first step in this study is to analyze the impact of the wind power plant location on the system frequency performance (e.g. measured by Nadir) in the frequency containment period. Besides, it is considered that each wind power plant has IE control with parameter values as defined in Table I. Fig. 6 illustrates the value of Nadir that results when each wind power plant performs IE.

TABLE I. PARAMETERS OF IE CONTROL FOR SENSITIVITY ANALYSIS.

Selected parameters	Value
$f_t$ [Hz]	49.95
$f_p$ [Hz]	49.70
$P_m$ [pu]	0.3
$T_{imx}$ [s]	15
$f_n$ [Hz]	50

As shown in Fig. 6, IE of WP2B entails the most noticeable improvement of Nadir. It is worth mention that this wind power plant is the biggest one and is close to the location where the imbalance is originated (i.e. outage of generator A1aG). Hence, it is inferred that the size and the distance of the wind power plant to the disturbance location influences the performance of IE control.

In the subsequent analysis, WP2B is considered to illustrate the tuning of a single wind power plant performing IE in the system. The parameters used as starting point for the parametric sensitivity based tuning of IE control are the given in Table I. As indicated in Fig. 4, one of the parameters is changed while the others remain fixed.

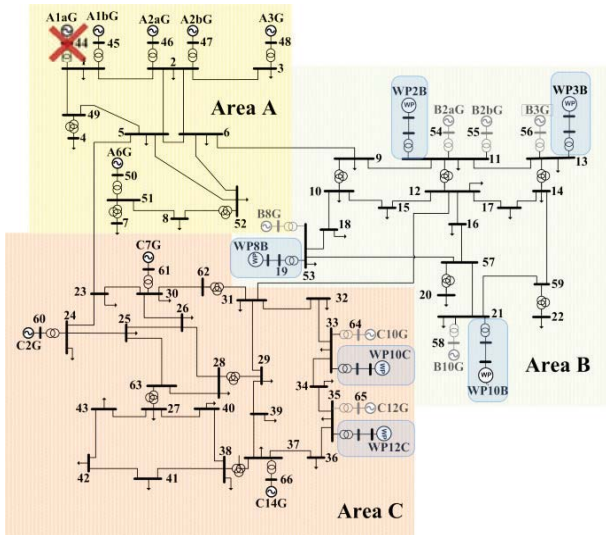


Figure 5. Three-area benchmark with WP integrations.

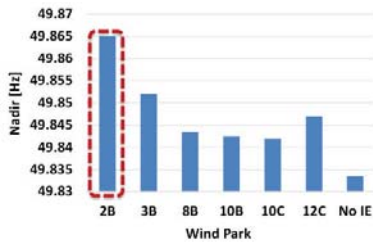


Figure 6. Nadir resulting when each wind power plants performs IE.

#### A. Activation time for IE controller

The activation process, as shown in Section II, is based on a comparator (cf. Fig. 3). The trigger signal will be generated by comparing the measured frequency to its reference value. IE control is activated when the sensed frequency deviation

reaches a predefined trigger value. In the application of the parametric sensitivity approach, the trigger value ( $f_t$ ) is varied between feasible ranges from 49.88 to 49.98 Hz, whereas the rest of the parameters have the values shown in Table I.

Figs. 7 and 8 show the frequency performance and the mechanical power of the wind turbine for different values of  $f_t$ . Following the triggering signal, the IE controller is activated and it is assumed it lasts for 15 s [11], [16].

Note in Fig. 9 that higher values of triggering signal for IE activation, especially higher than 49.87, will have better effect on the system frequency performance during the containment period. As a complementary part of this sub-section, additional comparison for different values of  $f_t$  is presented by Figure 10, when considering activation of IE in single wind power plant location as well as different combinations of wind power plants with activation of IE.

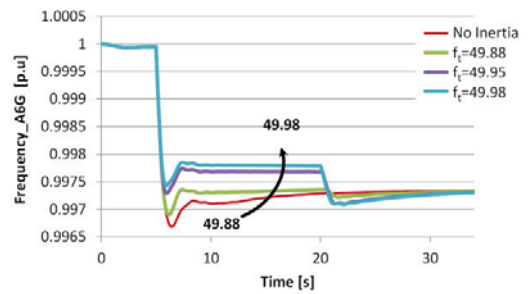


Figure 7. Frequency response for various values of activation trigger ( $f_t$ ).

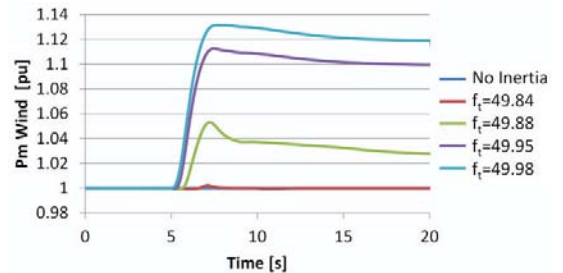


Figure 8. Mechanical power of wind turbine (W2B).

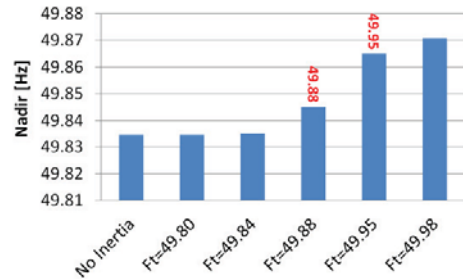


Figure 9. Nadir for different values of trigger  $f_t$ .

As shown in the figure 9 and 10, if the triggering time is set to 49.88 Hz or lower, the improvement in Nadir due to IE controller action will be limited, whereas there is a minor effect on RoCoF. Hence, a faster activation of IE controller is needed. This entails that higher values for the triggering, like 49.95 have to be chosen to enhance Nadir.

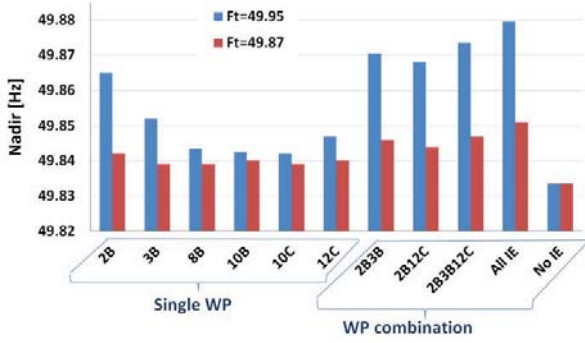


Figure 10. Nadir values for various WPs with different  $F_t$ .

### B. Threshold for maximum emulated power

As shown in Section II (cf. Fig. 3), there is an additional trigger ( $f_p$ ) for releasing the maximal allowed power by the IE controller. This action will happen if the frequency drop reaches a very low value, denoted here as  $f_{pinmax}$ . As shown in Figs. 11 and 12, this parameter is increased from 49.65 to 49.85. The higher value gives a better performance, which is due to maximal extraction of power. It should be mentioned that this value cannot be close or higher than  $f_t$ . This limitation is related to the equation (1), which might bring inappropriate gain with the unstable operation.

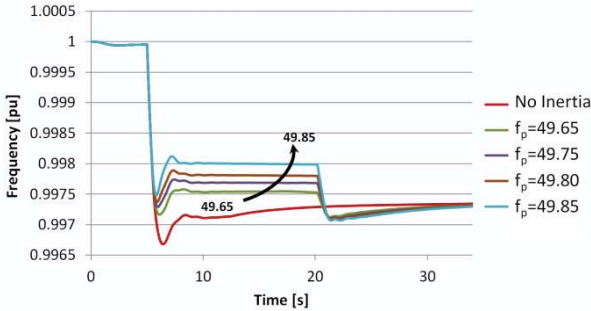


Figure 11. Frequency response for various values of maximal trigger  $f_p$ .

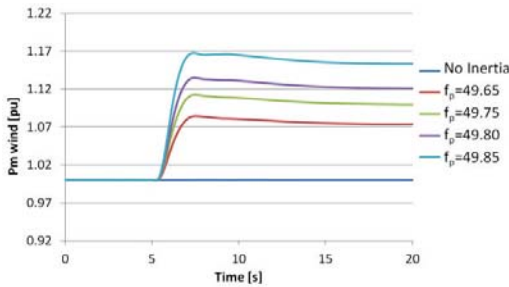


Figure 12. Mechanical power of wind turbine (W2B).

### C. Allowable additional power output

As shown in Section II (cf. Fig. 3), there is a proportional gain ( $P_m$ ) to limit the allowable additional power output from the wind turbine. This gain can be set to values up to 20% of the nominal wind turbine active power [11] and [16]. Therefore, the effects of this parameter, varies from 0.05 to

0.4, on the system performance is presented in Fig. 13. It shows that higher values lead to higher performance, but the physical limits of wind turbine can define the maximum value for this parameter.

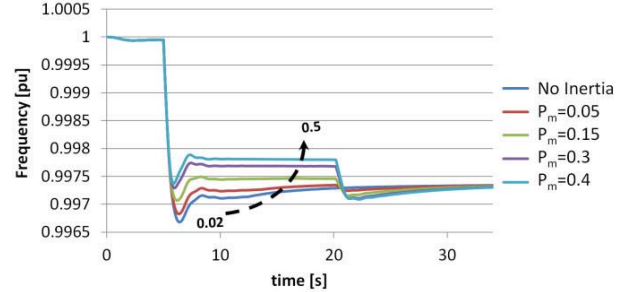


Figure 13. Frequency response for various values of  $P_m$ .

### D. Maximum duration for inertia emulation

The effects of inertia emulation time period are presented in Fig. 14. It is assumed that it ( $T_{imx}$ ) varies from 5 sec to 30 s. It is worth pointing out that depending on available energy, the normal range for time period is around 15-20 sec, but in this part of simulation this range is extended to show the effects of IE. Additionally, mitigating the first peak of the frequency increase/decrease after the occurrence of an imbalance can be defined as a priority, and the time duration for FFR (via IE control) can be adjusted depending of the available sources for frequency containment.

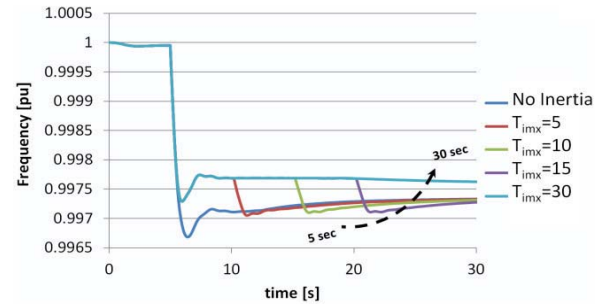


Figure 14. Frequency response for various periods of inertia emulation.

### E. Combination of multiple WP with IE capabilities

Ideally, it would be simply decided to required that all of wind power plants of a power systems have FFR capability. Nevertheless, it is worth evaluating if a minimum subset (combination) of wind power plants with IE can entail the satisfactory frequency performances as in the case when all wind power plants perform IE. Indeed, as shown in Fig. 15, the combination of WP2B, WP3B, WP12C has the highest and the most similar performance compared to the case that all the wind power plants actively perform IE.

The parameters of the IE of the three wind power plants selected to perform IE are given in Table II. This combination is kept for further analysis in terms of increasing the WP penetration in the whole grid.

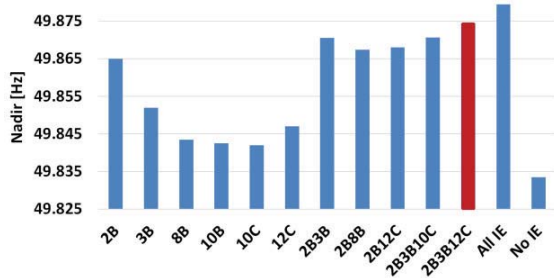


Figure 15. Nadir for different combinations of WP with IE controller.

TABLE II. PARAMETERS OF IE FOR DIFFERENT WIND POWER PLANTS.

Selected parameters	WP2B	WP3B	WP12C
$F_{trigger}$ [Hz]	49.95	49.95	49.95
$F_{pinmax}$ [Hz]	49.75	49.70	49.60
$P_{eminmax}$ [pu]	0.3	0.3	0.3
$T_{inx}$ [s]	50	50	50
$f_n$ [Hz]	50	50	50

#### F. Maximum penetration level

In this section, the effectiveness of IE when increasing the level of wind power penetration is evaluated. According to the ENTSO-E evaluation criteria, values of Nadir between 49.8 Hz and 50.2 Hz can be considered as limit during contingencies. As shown in Figure 16, within the existing controls, the maximum reachable penetration level is up to 50% for the 3-area test system. It is concluded that by means of properly tuning of IE control in key (selected) wind power plants, it is possible to ensure compliance of Nadir limit when increasing the penetration level of wind power generation (which is maximum 50 % in the case of the 3-area benchmark system).

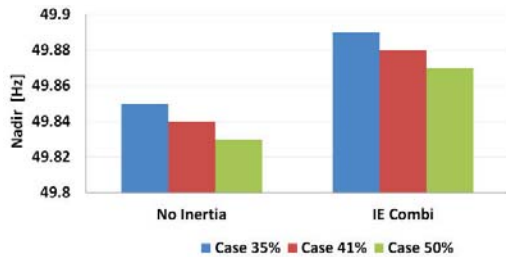


Figure 16. Nadir values for different wind power plant penetration with and without IE controllers.

## V. CONCLUSIONS

A sensitivity-based approach for evaluating the effects of FFR capabilities for wind turbine and to understand how the parameters of IE controllers can affect the system is presented and discussed. A complete set of analysis with recommended ranges for control parameters with a suitable methodology for defining the maximum achievable penetration level of wind turbines is performed. According to the obtained results, the activation time for IE controller will have direct effects on capturing the changes of Nadir. It should be mentioned that, the values of IE control parameters are tunable according to the nature of the power grid and available

sources. The study presented in this paper can be used as a guideline for system operators to investigate the best wind power plant combination with IE controllers and to identify the maximum achievable penetration level in large-scale interconnected power systems.

## ACKNOWLEDGMENT



This research was carried out as part of the MIGRATE project. This project has received funding from the European Union's Horizon 2020 research and innovation program under grant agreement No 691800. This reflects only the authors' views and the European Commission is not responsible for any use that may be made of the information it contains.

## REFERENCES

- [1] P. Tielens, D. Van Hertem, "The relevance of inertia in power systems," *Renewable and Sustainable Energy Reviews*, vol. 55, 2016.
- [2] R. Eriksson, N. Modig, K. Elkington, "Synthetic inertia versus fast frequency response: a definition," *IET Renewable Power Generation*, vol. 12, no. 5, pp. 507 – 514, 2018.
- [3] M. Dreidy, H. Mokhlis, S. Mekhilef, "Inertia response and frequency control techniques for renewable energy sources: A review," *Renewable and Sustainable Energy Reviews*, vol. 69, pp. 144–155, 2017.
- [4] F. Hafiz, A. Abdennour, "Optimal use of kinetic energy for the inertial support from variable speed wind turbines," *Renewable Energy*, vol. 80, pp. 629–643, 2015.
- [5] Gonzalez-Longatt F.M., "Effects of the synthetic inertia from wind power on the total system inertia: simulation study," *IEEE environment friendly energies and appl conference*; pp. 389–95, 2012.
- [6] H. Knudsen, J.N. Nielsen, *Introduction to the modelling of wind turbines: Wind Power in Power Systems*, Second Edition, 2005.
- [7] F. Gonzalez-Longatt, E. Chikuni, E. Rashayi, "Effects of the synthetic inertia from wind power on the total system inertia after a frequency disturbance," *Proceedings of IEEE Ind Technol Conference*, 2013.
- [8] S. Mishra, P. Zarina, P. Sekhar, "A novel controller for frequency regulation in a hybrid system with high PV penetration," *In: IEEE Power and Energy Soc General Meeting (PES)*, p. 1–5, 2013.
- [9] R. Josephine, S. Suja, "Estimating PMSG wind turbines by inertia and droop control schemes with intelligent fuzzy controller in Indian," *Dev J Elect Eng Technol*, vol. 9, pp. 1196–201, 2014.
- [10] W. Yao, K.Y. Lee, "A control configuration of wind farm for load-following and frequency support by considering the inertia issue," *Proceedings of IEEE Power and Energy Soc General Meeting*, 2011.
- [11] S. Engelken, A. Mendonca and M. Fischer, "Inertial response with improved variable recovery behaviour provided by type 4 WTs," *IET Renewable Power Generation*, vol. 11, no. 3, pp. 195–201, 2017.
- [12] C.C. Le-Ren, W.T. Lin, Y.C. Yin, "Enhancing frequency response control by DFigsin the high wind penetrated power systems," *IEEE Trans. Power Syst.*, pp. 710–718, May 2011.
- [13] M. Mauricio, A. Marano, A. Gómez-Expósito, J.L. Martínez Ramos, "Frequency regulation contribution through variable-speed wind energy conversion systems," *IEEE Trans. Power Syst.*, 2009.
- [14] Miao, L.L. Fan, "Wind farms with HVdc delivery in inertial response and primary frequency control," *IEEE Trans. Energy Convers.* pp. 1171–1178, December 2010.
- [15] MIGRATE Work Package 1 – responsible partner: TenneT, "MIGRATE Deliverable 1.1: Report on Systemic issues," MIGRATE consortium, 2016 ([www.h2020-migrate.eu](http://www.h2020-migrate.eu)).
- [16] J. Morren, W.H. de haan, Wil L. kling, J. A. Ferreira, "Wind Turbine Emulating Inertia and Supporting Primary Frequency Control," *IEEE Transactions on Power Systems*, vol. 21, No. 1, 2006.
- [17] J. L. Rueda, J. C. Cepeda, I. Erlich, A. W. Korai, and F. M. Gonzalez-Longatt, "Probabilistic approach for risk evaluation of oscillatory stability in power systems, in PowerFactory Applications for Power System Analysis," edited by F. M. Gonzalez-Longatt and J. Luis Rueda (Springer International Publishing, Cham, 2014) pp. 249–266.